Nondestructive pressure measurement of pressurized vessels via local magnetization and magnetic sensing

Huang Xinjing, Yan Yutian, Feng Hao *, Li Jian

State Key Laboratory of Precision Measuring Technology and Instruments, Tianjin University, Tianjin 300072, People's Republic of China
Binhai International Advanced Structural Integrity Research Centre, Tianjin 300072, People's Republic of China

ABSTRACT

This paper presents a nondestructive method for measuring the pressure of pressurized vessels through local magnetization (LM) and magnetic sensing. Firstly, tensile experiments of steel plates are carried out to character the magnetic sensitivity to plate stress with LM; It is demonstrated that the sensitivity to stress is higher when the magnet and magnetometer are fixed on different sides of the plate than that on the same side, and demagnetizing the steel plate can enhance the sensitivity. Then, pressure measurement comparison experiments on a pressurized vessel with and without optimized LM and magnetic measurement configurations are carried out to test the sensitivity and anti-interference ability of this method. It is demonstrated that LM can improve the magnetic sensitivity to vessel pressure by 2–3 times; LM can reduce the radial, circumferential and axial magnetic sensitivity fluctuations due to moving/rotating by 90.4%/94.4%, 96.5%/77% and 82.4%/87.4%.

© 2020 Elsevier Ltd. All rights reserved.

1. Introduction

Traditional pressure measurement methods for pressurized vessels require drilling a hole on the vessel, which destroys the structural integrity and strength of the vessel. Nondestructive pressure measurement does not require drilling to conduct the pressure into a pressure gauge, which can maintain the structural integrity of the pressurized vessel. Nondestructive pressure measurement methods mainly include strain gauge based method [1], optic fiber grating based method [2], capacitance measurement based method [3], and ultrasonic method [4]. Among them, the strain gauge and optic fiber grating based methods need to clean the coating on the surface of the vessel and need high quality bonding. In addition, optic fiber sensor requires costly light source and demodulator. The capacitive method has fast dynamic response and high sensitivity, but its measurement accuracy is extremely susceptible to electromagnetic interference. The ultrasonic method measures the pressure or stress of a pressurized vessel by measuring the velocity and amplitude changes of the acoustic or stress waves that propagate through the content inside or the wall of the vessel, but the deployment of acoustic transducer pair is complex and requires couplant.

According to the thin-wall stress theory of pressurized vessels, the wall stress of a vessel will increase as the internal pressure increases, and they have a linear proportional relationship [5]. The stress of a ferromagnetic material will significantly change the magnetic behavior of the material, such as magnetization state, magnetic permeability, magnetic anisotropy, Barkhausen noise, etc. These phenomena are called magneto-mechanical effects [6–8]. Magneto-mechanical effects have been widely used to assess the stress state or residual stress of steel structures, such as steel cables [9–11], steel strips [12–14], rails [15,16], pipelines [17,18], etc. The magneto-mechanical effect is a potential method for pressure measurement of pressurized vessels, although this has rarely been reported elsewhere.

For ferromagnetic pressurized vessels, under the magneto-mechanical effect, the magnetization state of the vessel wall will change under the combined effects of stress and ambient magnetic fields, which will cause the magnetic field around the vessel to change. Characterization of the change of the wall stress and/or the internal pressure by using the magnetic field change near the vessel surface has the advantages of being nondestructive, non-contact and simple layout.

Previously we proposed a nondestructive, non-contact pressure measurement method for pressurized vessels based on the magneto-mechanical effect, and demonstrated that the magnetic fields near the vessel surface can sensitively characterize the pressure changes in weak geomagnetic environment [19]. Because the

magnetic field is passively measured, the pressure measurement accuracy of this method is easily disturbed by the ambient magnetic field fluctuation, and measurement device needs to be recalibrated after the pressurized vessel is moved or rotated. Against this drawback, this paper proposes to utilize active local magnetization (LM) to improve the magnetic sensitivity and anti-interference ability of pressure measurement based on the magneto-mechanical effect.

Firstly, this paper investigates the sensitivity of near-surface magnetic flux density to the stress of steel plates when the plate is subjected to strong local magnetization (LM) via tensile tests. In order to optimize the magnetic measurement configurations, several relevant factors are investigated including the layout of the magnet and the magnetometer, measuring point locations, and the effect of demagnetization on the sensitivity. Then, the magnetic sensitivity and anti-interference ability of pressure measurement of a pressurized vessel with the optimized configuration are compared with the method without LM. The second group of tests include sensitivity enhancement tests for many randomly distributed measuring points, and anti-interference ability tests by moving and rotating the vessel to change the magnitude and direction of the ambient magnetic field and hence induce magnetic interferences.

2. Feasibility verification via tensile tests of steel plates

Tensile tests of steel plates were carried out to determine the optimal configuration including magnet and magnetometer layout, measuring point locations and demagnetization. Tensile test apparatus is shown in Fig. 1. Two t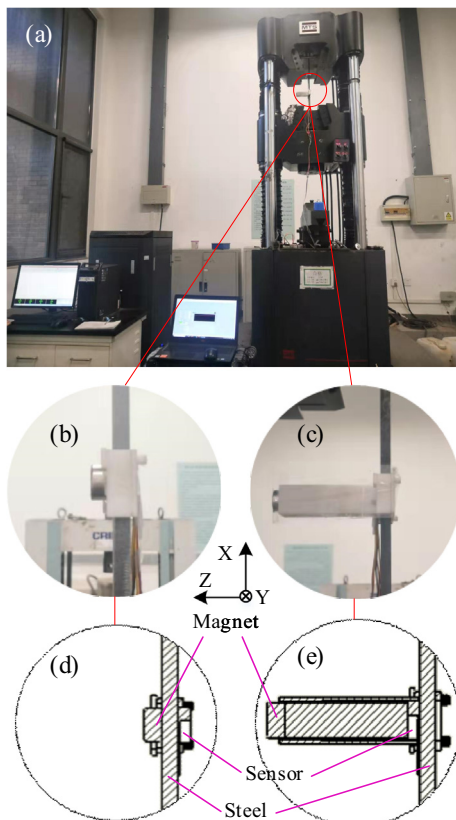ypes of experiments were carried out for each steel plate: A-- the magnet and the magnetometer are attached on the same side of a steel plate to be tested; and B-- the magnet and the magnetometer are attached on two different sides of the plate. In type A experiment, the magnet and the magnetometer are separated with a large interval to prevent the magnetometer from saturation. In this case, the magnet cannot firmly hold the plate by itself, so a clamping device was used. In type B experiment, a 2 mm spacer was placed between the magnet and the plate, so the magnet can firmly hold the plate by itself; the magnetometer was stuck in the mirror-symmetrical position on the other side of the test piece. Dimension drawings and photos of the tested steel plates are shown in Fig. 2(a). Two thicknesses of steel plates were tested, 1: T = 5 mm and 2: T = 7.5 mm. Wall thickness of the pressurized vessel used in the subsequent experiment is also 7.5 mm. Steel plates are numbered by combining the thickness number and the test order. For example, 1–3 plate is the third 5 mm thick steel plate.

In the tensile test, the tensile force was increased at a speed of 1 kN/s, and the triaxial magnetic flux density near the surface of the steel plate were collected at the same time. The specimens with T = 5 mm and T = 7.5 mm were loaded to 50kN and 75kN respectively, and both of their maximum tensile stresses were 167 MPa. In type A and B experiments, each steel plate was linearly stretched from 0 to 167 MPa for three times to eliminate irreversible magnetization. One typical stress/strain curve of the sample in the tensile test is shown in Fig. 2(b). Both the stress and strain linearly change as a function of time, which means that during this process, the specimens were all in the stage of elastic deformation. Change amount of the magnetic flux density detected by the magnetometer during the third stretching process is taken as the magnetic sensitivity to the stress, and the results are summarized in Fig. 3. After demagnetizing these steel plates, tensile tests were performed again to obtain the magnetic sensitivity to stress, and the results are shown in Fig. 4. Demagnetized samples 1–3 and 2–3 were destroyed due to the accidental control-losing failure of the
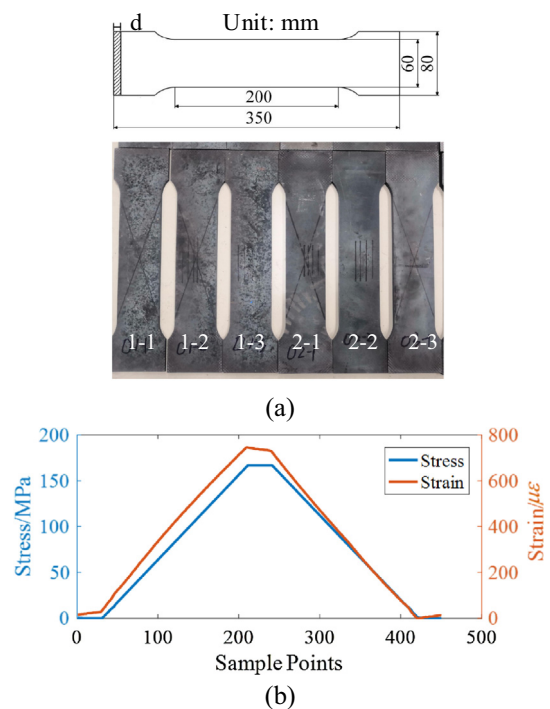

Fig. 1. Tensile test apparatus for steel plates: (a) tensile test machine; (b) (d) type B experiment, the magnet and the magnetometer are attached at different sides; (c) (e) type A experiment, the magnet and the magnetometer are placed at the same side.

Fig. 2. Information about the tested steel plates: (a) Dimension drawing and photos of tested steel plates; (b) One typical stress–strain curve of the sample in the tensile test.
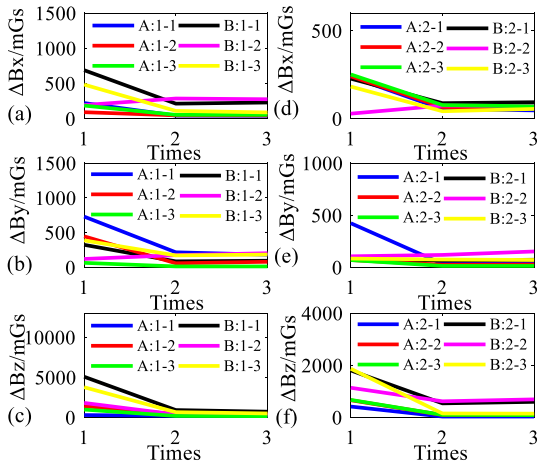
Fig. 3. Summary of the magnetic sensitivity to stress before the steel plates are demagnetized: (a)-(c) steel plates with T = 5 mm, (d)-(f) steel plates with T = 7.5 mm.
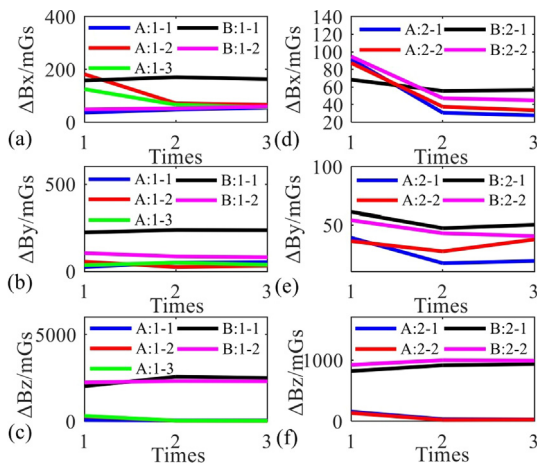

Fig. 4. Summary of the magnetic sensitivity to stress after the steel plates are demagnetized: (a)-(c) steel plates with T = 5 mm, (d)-(f) steel plates with T = 7.5 mm.

tensile test machine. These sets of data are invalid, and therefore not included. The raw data of all the curves in Figs. 3 and 4 is put in the supplementary material file.

It can be seen from Fig. 3 and Fig. 4 that whether demagnetizing the steels or not, the sensitivity of each magnetic component to stress is greater when the magnet and magnetometer are distributed at different sides of the plate (type B experiment) than that when the magnet and magnetometer are distributed at the same side (type A experiment). The sensitivity of normal component B_z to stress is greater than that of the other two tangential components (B_x and B_y). For type B configuration, when the steel plate is demagnetized, the sensitivity of B_z to stress is 1000–2000mGs, which is much higher than that when the steel plate is not demagnetized. For type B configuration, the sensitivity of B_z to stress is 1000mGs higher than that of type A configuration. Therefore, in the pressure measurement experiment, in order to obtain higher sensitivity, the pressurized vessel should be demagnetized, and the magnetometer and the magnet should be placed on different sides of the vessel wall.

The raw data of all the curves in Figs. 3 and 4 is put in the supplementary material file. It is worth noting from the raw data that the curves of the near-surface magnetic flux density as a function of the increasing stress are not all monotonic, and the extreme

points of the non-monotonic curves appear between about 40 MPa and 100 MPa. Therefore, internal pressure measurement of the vessel based on the magneto-mechanical effect with LM can only be implemented in low pressure range. For example, the thickness t of the pressurized vessel used in subsequent experiments is 7.5 mm, and its diameter D is 275 mm, height H is 300 mm. Its allowable pressure $p \in [0, 3 \text{ MPa}]$, so the hoop stress $\sigma_c = pD/(4t) = 9.2p \leqslant 27.6$ MPa and the axial stress $\sigma_a = pDH/(2(D + H)t) = 9.6p \leqslant 28.8$ MPa; both of them are below the extreme points and p is in the monotonic interval of pressure measurement.

3. Pressure measurement experiments

Experimental apparatus for measuring the pressure of a pressurized vessel with LM is shown in Fig. 5(a). A pressure pump injects water into the pressurized vessel, a pressure regulator controls the pressure inside the vessel, and a high-precision pressure gauge is used to display the pressure. Several identical magnets are adsorbed at 18 different positions on the inner surface of the vessel, and the magnetometers are fixed outside the vessel opposite to the magnets. Then magnetic sensitivity to the pressure at different positions was tested. Measurement points were randomly distributed, and approximate heights and circumferential positions are shown in Fig. 5(b). During the pressure measurement experiments, firstly, the vessel was pressurized to its allowable pressure 3 MPa by the pump, and then the pump was closed and the regulator was opened to a small aperture to slowly release the pressure to 0 MPa. During the entire pressure adjustment process described above, the magnetometers were recording triaxial magnetic signals.

Contrast test of pressure measurement based on the magneto-mechanical effect without LM was carried out. The experiment apparatus is shown in Fig. 6, which is the same as that in [19]. There are 10 magnetometers, and the height of the measurement points is adjusted by a lifting structure. Magnetometers measure the triaxial magnetic components around the container: radial, circumferential, and axial magnetic flux densities, denoted by B_r, B_c, and B_a, respectively. The FPGA (Field Programmable Gate Array) controller synchronously collects magnetic signals of all the magnetometers through the IIC (Inter-Integrated Circuit) bus, and transmits them to a personal computer via USB for saving and displaying. Pressure regulation process of the vessel is in the same
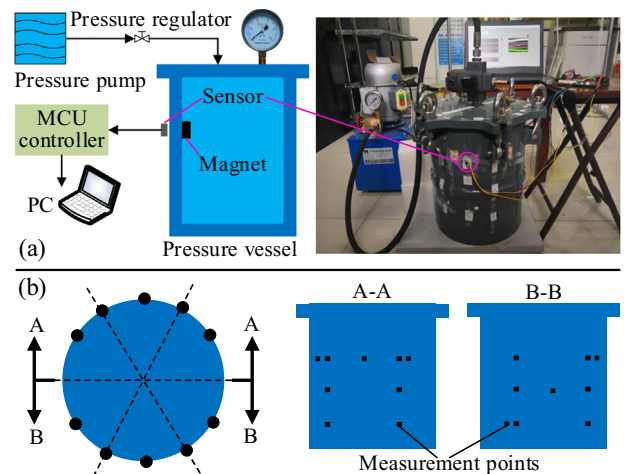

Fig. 5. Experiments for measuring the pressure of the pressurized vessel with LM: (a) schematic and photo of experimental apparatus; (b) diagrammatic drawing of random distribution of measurement points.
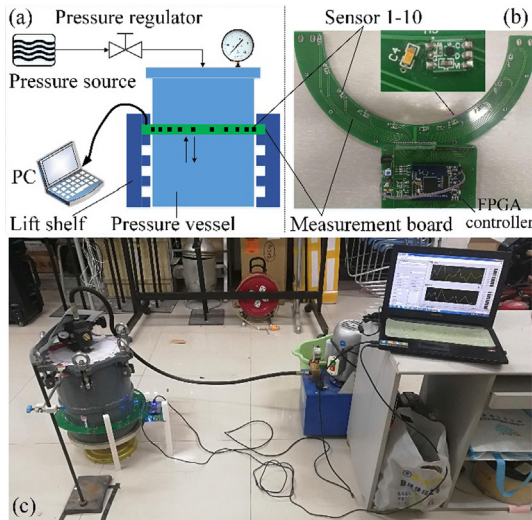
Fig. 6. Experiment for measuring the pressure of the pressurized vessel immersed in weak geomagnetic fields: (a) schematic of experiment apparatus; (b) measurement devices; (c) experiment photo.

way as that tests with LM. In the experiment, the measurement board was moved to three heights: the upper, middle, and lower parts of the pressurized vessel, as shown in Fig. 6(a). Each time when the height was adjusted, the vessel was pressurized to 3 MPa first and then released to 0 MPa. Pressurization and releasing were repeated three times for three height. At each height, 10 magnetometers measure the triaxial magnetic components around the container, so $3 \times 10 \times 3$ curves of B_r, B_c, and B_a vs pressure were obtained.

Contrast tests above can determine whether the pressure measurement of pressurized vessels with LM based on the magneto-mechanical effect is feasible and whether the LM can generally improve the sensitivity of pressure magnetic measurement at different measurement points. In addition, as shown in Fig. 7, pressure magnetic measurements of the pressurized vessel in the weak geomagnetic environment without and with LM are tested and compared via moving and rotating the vessel in the laboratory to determine whether LM can enhance the anti-interference ability.

4. Results and discussions

4.1. Sensitivity

Test results of the magnetic flux density vs the pressure at 30 measurement points near the surface of the pressurized vessel
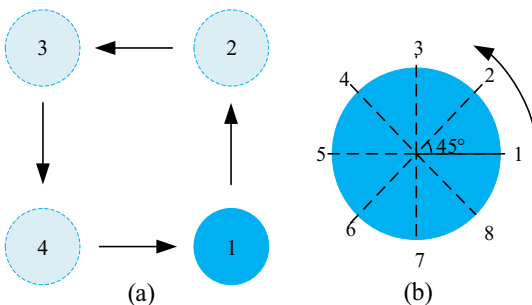

Fig. 7. Anti-interference ability tests of pressure magnetic measurement with and without LM by moving (a) and rotating (b) the pressurized vessel.

without LM are shown in Fig. 8, and Fig. 8(a)-(c) are the radial, circumferential, and axial magnetic flux density, respectively. To calculate the magnetic sensitivity to pressure, only the initial/final magnetic flux density and pressure are required, so the pressure as a function of time was not recorded. The pressure variations from the initial 3 MPa to the final 0 MPa are all identified and known. For the convenience of comparison, different measurement curves have their own initial values subtracted and the magnetic flux density shifts are presented. The pressure was released at 10 s. Curves 1–10, 11–20, and 21–30 are the test results of 10 measurement points located at the upper, middle, and lower parts of the pressurized vessel, respectively. The change in magnetic flux density at these 30 points is divided by the change in pressure to get the sensitivity of each point as well as the maximum and average sensitivity of the three magnetic components; the results are listed in Table 1. S_r, S_c, and S_a represent the magnetic sensitivity in the radial, circumferential, and axial directions, respectively.

Test results of the magnetic flux density vs the pressure at 18 measurement points near the surface of the pressurized vessel with LM are shown in Fig. 9, and Fig. 9(a)-(c) are the radial, circumferential and axial magnetic flux density, respectively. For the convenience of comparison, different measurement curves have their own initial values subtracted and the magnetic flux density shifts are presented. The pressure was released at 10 s. The approximate positions of each measurement point are shown in Fig. 5(b). The change in the magnetic flux density at these 18 points is divided by the change in pressure to get the sensitivity of each point as well as the maximum and average sensitivity of the three magnetic components; the results are as listed in Table 2. S_r, S_c, and S_a
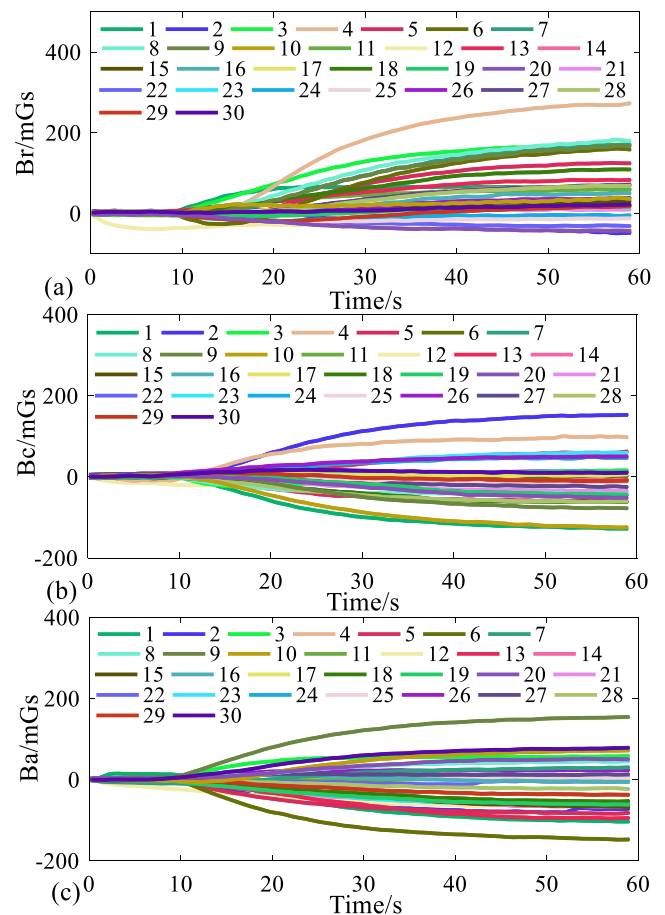

Fig. 8. Measurement results of magnetic sensitivity to pressure at different measurement points on the vessel surface without LM.

Table 1
Summary of sensitivities of each measurement point on the vessel surface without LM, unit: mGs/MPa.

No.	S_r	S_c	S_a
1	22.45	46.08	41.33
2	23.53	55.43	29.34
3	59.18	15.22	19.52
4	97.67	37.77	15.41
5	47.27	21.19	29.86
6	66.59	3.66	51.88
7	61.11	19.33	14.33
8	63.62	15.06	16.44
9	59.74	29.99	53.45
10	14.10	45.55	27.12
11	19.72	3.69	2.51
12	14.80	12.72	22.36
13	27.00	20.37	32.65
14	25.02	4.25	23.01
15	13.00	5.55	23.52
16	19.45	4.69	5.92
17	25.59	3.61	18.34
18	36.86	21.19	19.14
19	8.43	15.56	21.69
20	13.90	17.75	16.26
21	5.11	12.68	21.16
22	10.55	5.89	4.44
23	7.91	20.05	20.74
24	6.34	15.57	19.56
25	6.62	6.05	4.58
26	15.99	17.02	8.27
27	25.27	11.21	5.51
28	24.32	21.70	7.53
29	12.90	7.64	13.45
30	7.40	5.78	26.59
Average	28.05	17.41	20.53
Maximum	97.67	55.43	53.45

Fig. 9. Measurement results of magnetic sensitivity to pressure at different measurement points on the vessel surface with LM.

Table 2
Summary of sensitivities of each measurement point on the vessel surface with LM, unit: mGs/MPa.

No.	S_r	S_c	S_a
1	28.97	27.77	42.97
2	−32.17	−56.53	29.77
3	99.27	−66.83	33.70
4	−11.27	18.97	−36.13
5	82.43	99.10	29.17
6	−51.13	−33.77	−18.27
7	−75.13	121.33	−174.40
8	−173.00	−35.20	40.50
9	31.73	−54.17	15.27
10	−151.07	21.70	−67.37
11	−210.87	82.13	175.33
12	206.43	−92.87	54.37
13	−43.13	−47.83	35.00
14	46.07	100.10	−17.73
15	51.10	−98.13	11.23
16	−86.27	66.90	−61.33
17	52.57	−16.27	−23.43
18	24.73	64.10	−26.67
Average	80.96	61.32	49.59
Maximum	210.87	121.33	175.33

represent the magnetic sensitivity in the radial, circumferential, and axial directions, respectively.

It can be seen from Fig. 8 and Fig. 9 that the three magnetic components at each measurement point change as the pressure in the vessel changes, whether with LM or not. The sensitivities at different measurement points are quite different, and being positive or negative is also uncertain. Comparing Fig. 8 and Fig. 9, it can be seen that when the change of pressure in the vessel is the same, the change of magnetic flux density when LM is used is larger than that under weak geomagnetic environment with no LM. More specifically, comparing the sensitivities in Table 1 and Table 2, it can be seen that the average and maximum sensitivities of the three magnetic components when LM is used are significantly higher than that under the weak geomagnetic environment with no LM, and the former are about 2 to 3 times larger than the latter.

In the experiments of pressure measurement for the vessel with LM, there are noticeable differences in sensitivity at different measurement points, which are caused by the residual stress and residual magnetization on the pressurized vessel itself. As can be seen from Table 2, the sensitivity of the point 11 is the highest among the 18 measurement points, so it is taken as the best measurement point. Then the magnets and magnetometer are placed at point 11 to test whether the sensitivity is affected by movement and rotation of the pressurized vessel.

4.2. Anti-interference ability

The anti-interference ability of the proposed method based on LM was tested by moving and rotating the pressurized vessel. Moving the vessel can change the nearby ambient magnetic field, while rotating the vessel can change the direction of the magnetization by the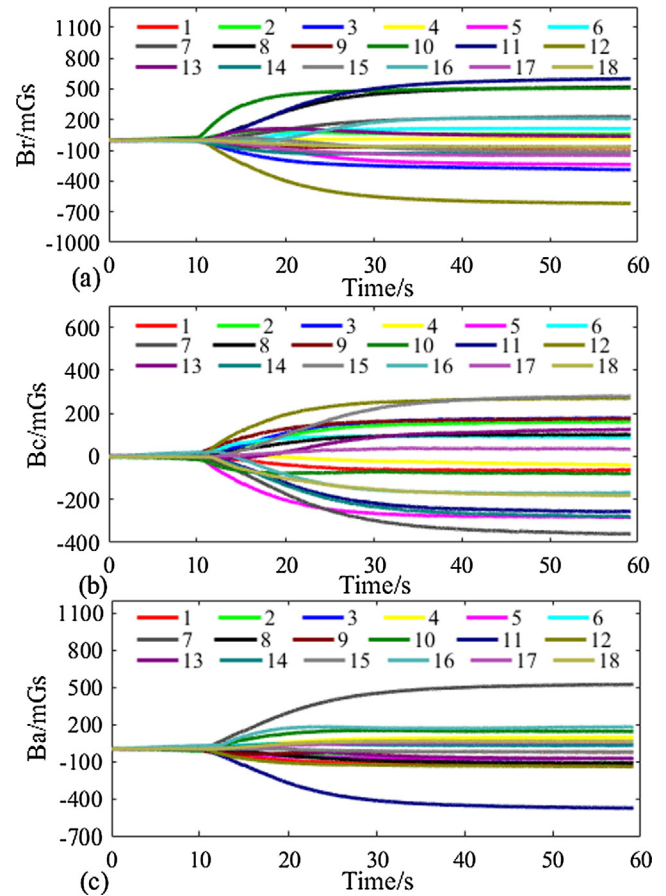 ambient field to the vessel. The magnet and the magnetometer ① were arranged at the measurement point No.11. In addition, a set of contrast tests were carried out by attaching the magnetometer ② to the outer surface of the pressurized vessel far from the magnet where there is no LM except for weak geomagnetic magnetization. During the test, the pressurized vessel was first pressurized to 3 MPa, then the pressure regulator began to reduce the pressure with an interval of 0.5 MPa. Each

pressure was maintained for a duration of several seconds, during which the pressurized vessel was moved to four different positions in the laboratory (moved from position 1 to position 4 in the order as shown by the arrows in Fig. 7(a). and rotated by eight angles (rotated from angle 1 to angle 8 in the order as shown by the arrow in Fig. 7(b). At each position and each orientation mentioned above, the magnetic flux densities of the magnetometers ① with LM and ② without LM were measured, respectively. Average and standard deviation of the magnetic signals at each place were calculated, and the results are shown in Fig. 10 and Fig. 11. Among them, (a)-(c) are the data with LM, while (d)-(f) are the data with no LM.

It can be seen from Fig. 10 and Fig. 11 that the sensitivity with LM is much higher than that under weak geomagnetic magnetization without LM. Fluctuations of the triaxial magnetic components with LM when the position and direction of the vessel change are significantly smaller than that without LM. Under LM, the anti-interference ability of the magnetic flux density characterizing pressure is significantly enhanced. However, under LM, changes in vessel position and direction will in some extent still affect the pressure measurement accuracy. Specifically, the position change has a small effect on the sensitivity of the circumferential and axial magnetic components and a relatively large effect on the sensitivity of the radial component. The change in direction has a large impact on the sensitivity of the radial and circumferential magnetic components, and a small effect on the sensitivity of the axial component, because rotation does not change the orientation of the magnetometer in the axial direction.

Due to large differences in variation of the magnetic value, raw magnetic fluctuations for a fixed pressure value cannot truly reflect the pressure measurement accuracy. Therefore, relative fluctuation coefficient $C_i = \widetilde{B}_i / \Delta B_i$ is defined and used to express the fluctuation intensity of the measurement results caused by movement and rotation. Wherein, $i = r$, c, and a denoting radial, circumferential, and axial directions, respectively. $\widetilde{B}_i$ represents the standard deviation and ΔB_i represents the magnetic variance when the pressure changes by 3 MPa. A larger C_i means a more severe fluctuation. The calculation results are shown in Table 3. For movement, LM
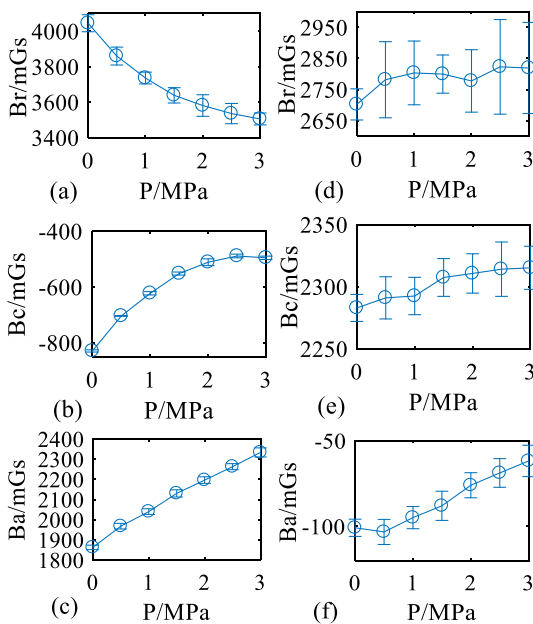

Fig. 11. Effect of rotating the vessel on pressure magnetic characterization: (a) (b) (c), with LM; (d) (e) (f), contrast group without LM, the vessel is immersed in weak geomagnetic fields.
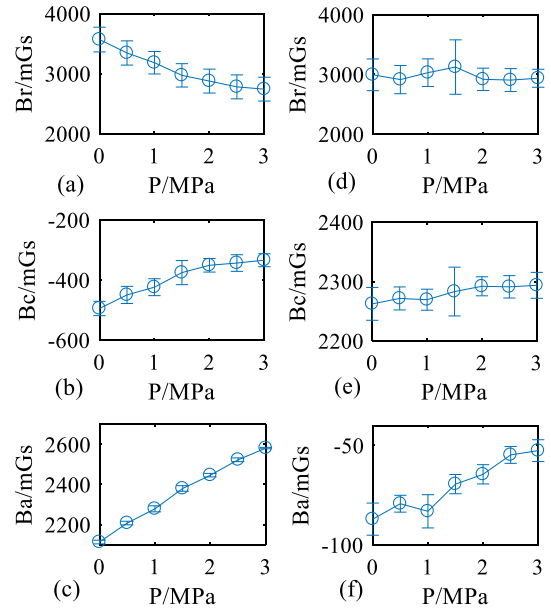
Table 3
Effects of movement and rotation on the fluctuations of magnetic measurement results.

Magnetic component		With LM①	Without LM②	①/②
Move the vessel	$\widetilde{B}_r / \Delta B_r$	0.0864	0.8972	9.6%
	$\widetilde{B}_c / \Delta B_c$	0.0177	0.5008	3.5%
	$\widetilde{B}_a / \Delta B_a$	0.0335	0.1910	17.6%
Rotate the vessel	$\widetilde{B}_r / \Delta B_r$	0.2398	4.2648	5.6%
	$\widetilde{B}_c / \Delta B_c$	0.1711	0.7437	23.0%
	$\widetilde{B}_a / \Delta B_a$	0.0209	0.1663	12.6%

reduces radial fluctuations by 90.4%, circumferential fluctuations by 96.5%, and axial fluctuations by 82.4%. For rotation, LM reduces radial fluctuations by 94.4%, circumferential fluctuations by 77%, and axial fluctuations by 87.4%. The experimental results demonstrate that LM can complete the pressure magnetic measurement of the pressurized vessel, and can effectively reduce the magnetic interference on the pressure measurement results due to the change of the position and orientation of the vessel.

5. Conclusions

This paper proposes to utilize LM to improve the sensitivity and anti-interference ability of nondestructive pressure measurement of pressurized vessels based on the magneto-mechanical effect. Firstly, the sensitivity of the near-surface triaxial magnetic field to the stress of the steel plate with LM is investigated by tensile tests of steel plates. The results demonstrate that in order to obtain higher sensitivity, the pressurized vessel should be demagnetized, and the magnetometer and the magnet should be placed on different sides of the steel plate and the vessel wall. Then, the magnetic sensitivity and anti-interference ability of pressure measurement of a pressurized vessel with and without LM are experimentally tested and compared using the optimized magnetization and magnetic measurement configuration.

Fig. 10. Effect of moving the vessel on pressure magnetic characterization: (a) (b) (c), with LM; (d) (e) (f), contrast group without LM, the vessel is immersed in weak geomagnetic fields.

It is demonstrated that LM can improve the average and maximum magnetic sensitivity to the vessel pressure by 2–3 times compared with passive magnetic measurement without LM, although the sensitivity at different measurement points varies greatly. When the vessel is moved/rotated, LM can reduce the sensitivity fluctuation of the radial magnetic component by 90.4%/94.4%, reduce the sensitivity fluctuation of the circumferential magnetic component by 96.5%/77%, and reduce the sensitivity fluctuation of the axial magnetic component by 82.4%/87.4%. Therefore, LM can significantly improve the sensitivity and anti-interference ability compared with the pressure magnetic measurement based on the magneto-mechanical effect without LM.

CRediT authorship contribution statement

Huang Xinjing: Methodology, Funding acquisition, Writing - review & editing, Project administration. **Yan Yutian:** Data curation, Validation, Software. **Feng Hao:** Conceptualization, Resources, Project administration. **Li Jian:** Funding acquisition, Project administration.

Declaration of Competing Interest

The authors declare that they have no known competing financial interests or personal relationships that could have appeared to influence the work reported in this paper.

Acknowledgments

Appendix A. Supplementary material

Supplementary data to this article can be found online at https://doi.org/10.1016/j.measurement.2020.107993.

References

[1] A.M. Sadeghioon, N. Metje, D.N. Chapman, et al., Wireless Sensor Network Based Pipeline Failure Detection System Using Non-intrusive Relative Pressure and Differential Temperature Measurements, ICE Publishing, Cambridge, United kingdom, 2016, pp. 173–178.

[2] D. Nannan, W. Sumei, J. Lan, et al., Pressure and temperature sensor based on graphene diaphragm and fiber bragg gratings, IEEE Photonics Technol. Lett. 30 (5) (2018) 431–434.

[3] L. Shi-Yu, L. Jian-Gang, et al., Influence of permittivity on the sensitivity of porous elastomer-based capacitive pressure sensors, IEEE Sens. J. 18 (5) (2018) 1870–1876.

[4] L. WeiBin, Research on Pressure Measurement Model Based on Ultrasonic Wave, Master dissertation, Zhejiang University, Hangzhou, China, 2017.

[5] L. Hongwen, Plate Shell Theory, Zhejiang University Press, Hangzhou, China, 1987, pp. 243–271.

[6] D.C. Jiles, Theory of the magnetomechanical effect, J. Phys. D (Appl. Phys.) 28 (8) (1995) 1537–1546.

[7] J. Pearson, P.T. Squire, M.G. Maylin, et al., Biaxial stress effects on the magnetic properties of pure iron. IEEE, USA, vol. 36, no. 5, 2000, pp. 3251–3253.

[8] C.H. Gur, Review of residual stress measurement by magnetic barkhausen noise technique, Mater. Perform. Charact. 7 (4) (2018) 21.

[9] D. Dongge, W. Xinjun, Z. Su, A steel wire stress measuring sensor based on the static magnetization by permanent magnets, Sensors 16 (10) (2016) 1618–1650.

[10] S. Zhang, J. Zhou, Y. Zhou, et al., Cable tension monitoring based on the elasto-magnetic effect and the self-induction phenomenon, Materials 12 (14) (2019).

[11] Junkyeong Kim, Seunghee Park, Field applicability of a machine learning–based tensile force estimation for pre-stressed concrete bridges using an embedded elasto-magnetic sensor, Struct. Health Monitor. 19 (1) (2019) 281–292.

[12] G. Ben, Z. Yong, H. Xiaohui, et al., Cold-rolled strip steel stress detection technology based on a magnetoresistance sensor and the magnetoelastic effect, Sensors 18 (5) (2018) 1616–1638.

[13] Z. Qingdong, S. Yuanxiao, Z. Liyuan, et al., Magnetoelastic effect-based transmissive stress detection for steel strips: theory and experiment, Sensors 16 (9) (2016) 1317–1382.

[14] Y. Maeda, S. Urata, H. Nakai, et al., Development of the apparatus for measuring magnetic properties of electrical steel sheets in arbitrary directions under compressive stress normal to their surface, AIP Adv. 7 (5) (2017).

[15] M.K. Devine, Detection of stress in railroad steels via magnetic property measurements, Nondestructive Test. Evaluat. 11 (4) (1994) 215–234.

[16] S. Santa-Aho, A. Sorsa, A. Nurmikolu, et al., Review of railway track applications of Barkhausen noise and other magnetic testing methods, Insight - Non-Destructive Test. Condition Monitor. 56 (12) (2014) 657–663.

[17] Ortega-Labra Omar, Manh Tu Le, P. Martinez-Ortiz, et al., A novel system for non-destructive evaluation of surface stress in pipelines using rotational continuous magnetic Barkhausen noise, Measurement 136 (2019) 761–774.

[18] B. Liu, S. Zheng, L. He, et al., Study on internal detection in oil-gas pipelines based on complex stress magneto-mechanical modeling, IEEE Trans. Instrument. Measur. (2019) https://ieeexplore.ieee.org/document/8915729.

[19] Z. Zeng, C. Zhao, X. Huang, et al., Non-invasive pressure measurement based on magneto-mechanical effect, Measur. Sci. Technol. 29 (9) (2018).